

Low-mobility charge carriers in CuO

A. A. Samokhvalov, N. A. Viglin, B. A. Gizhevskii, N. N. Loshkareva, V. V. Osipov, N. I. Solin, and Yu. P. Sukhorukov

Institute of Physics of Metals, Ural Branch of the Russian Academy of Sciences

(Submitted 20 June 1991; revised 17 April 1992)

Zh. Eksp. Teor. Fiz. **103**, 951–961 (March 1993)

To establish the nature of conductivity in the quantum antiferromagnetic semiconductor CuO, which lies at the base of high- T_c superconductors, we study the kinetic and optical properties of CuO, namely, the electrical conductivity (dc, in the frequency range 10^4 – 10^7 Hz, and at 9.2 GHz), thermopower, the Hall effect, magnetoresistance, the absorption and reflection coefficients and light-induced conductivity in the infrared range of the spectrum, and the current-voltage characteristics and their first derivatives of the tungsten–CuO microjunction structure. The temperature range used in measurements, 80–400 K, incorporates both the antiferromagnetic region for CuO and the region of a quantum spin liquid for $T > T_{N_1} \approx 230$ K. Considerable variation in the conduction activation energy is observed at T_{N_1} . The results suggest a strong localization of the carriers (holes) in CuO, and can be described satisfactorily within the model of low-mobility localized carriers of the small-polaron type. We also discuss the possible role of electron-magnon coupling (besides the electron-photon mechanism) in the additional localization of carriers in CuO.

Among the possible hypotheses concerning the nature of high- T_c superconductivity, attention has been drawn to the role played in this phenomenon by electron-phonon and electron-magnon interactions, for instance, the t - J model (see Refs. 1 and 2). In this connection it would be interesting to study a whole range of electrical, optical, magnetic, and other physical properties of the antiferromagnetic semiconductor CuO, which lies at the core of the main group of high- T_c superconductors. The few reported studies of CuO show that many of its fundamental physical properties remain unchanged or change little in systems based on this compound: $\text{YBa}_2\text{Cu}_3\text{O}_x$ as $x \rightarrow 6$ and $\text{La}_{2-y}\text{Sr}_y\text{CuO}_4$ as $y \rightarrow 0$. For instance, the identical features of the infrared spectra of light-induced conductivity in CuO and $\text{YBa}_2\text{Cu}_3\text{O}_x$ (for $6 \leq x \leq 7$) may attest to the presence of low-mobility carriers (in addition to mobile carriers for $\text{YBa}_2\text{Cu}_3\text{O}_x$ as $x \rightarrow 7$) in both compounds.^{3,4}

Magnetically, CuO and $\text{YBa}_2\text{Cu}_3\text{O}_x$ with $c \leq 6.4$ and $\text{La}_{2-y}\text{Sr}_y\text{CuO}_4$ with $y \rightarrow 0$ are close in their properties as low-dimensional antiferromagnets.^{5,6} At the same time the low concentration of carriers in CuO in comparison with high- T_c superconductors makes it possible to employ optical methods to study in more detail a number of properties of CuO and specific features of its electronic structure, which are masked by the high metallic conductivity in typical high- T_c superconductors. It is also known that CuO is a quantum antiferromagnet with $T_{N_1} \approx 230$ K. A helicoid magnetic structure is observed in the $T_{N_1} \approx 230$ K to $T_{N_2} \approx 212$ K range, while below T_{N_2} CuO is a collinear antiferromagnet.^{6,7} Above T_{N_1} the state of a quantum spin liquid sets in. The small spin of the Cu^{2+} ion and, respectively, the quantum nature of the antiferromagnetism in CuO are the reasons why for CuO is quite different in its properties from the majority of antiferromagnetic (Néel-type) transition-metal oxides (such as NiO, for example). In this connection the study CuO is of interest from the standpoint of the physics of magnetism.

Bearing in mind the aforesaid and wishing to obtain

information about the nature of the conduction, the electronic structure, and the possible effect of magnetism on the kinetic properties of CuO, we undertook the study of a whole range of kinetic and optical properties of CuO. The temperature range used in measurements, 80–400 K, incorporates both the region of antiferromagnetic ordering in CuO with $T_{N_1} \approx 230$ K and the region of a quantum spin liquid for $T > T_{N_1}$.

SAMPLES AND MEASURING METHODS

Single crystals of CuO grown from a solution in a melt constitute prisms elongated along the c axis and as big as $12 \times 3 \times 2$ mm³. Polycrystals of $\text{Cu}_{1-x}\text{Li}_x\text{O}$ ($0 \leq x \leq 0.05$) were prepared from analytically pure CuO and La_2CO_3 powders by annealing and caking in an air atmosphere at 950 °C. The crystal lattice of CuO is monoclinic with the following typical parameters: $a = 4.72$ Å, $b = 3.40$ Å, and $c = 5.04$ Å. The angle between the a and c axes is 99.5°.

Conductivity measurements were carried out in the dc and ac modes in the 5×10^4 – 3×10^7 Hz frequency range and at a microwave frequency of 9.2 GHz. Attempts were made to measure the Hall effect and magnetoresistance in CuO in the dc mode and at $H \leq 20$ kOe. Also we measured the temperature dependence of the thermopower. The dc conductivity measurements were done by the usual four-point probe method, the ac measurements by employing a Q -meter, and the microwave measurements by the cavity method. Indium contacts were implanted by an ultrasound soldering iron. The optical measurements of the absorption and reflection coefficients (and, respectively, the light-induced conductivity) were conducted in the infrared spectra range ($\lambda = 0.7$ – 14 μm) using a modernized IKS-21 spectrometer at 300 and 80 K. We also studied the current-voltage characteristics and their first derivatives of a tungsten-needle–CuO-plane microjunction structure. It is well known that ballistic carrier motion can be achieved in a microjunction structure.⁸ In this mode a carrier acquires an energy eU cor-

responding to the potential U applied to the metal electrode and can activate energy transitions (direct or indirect) in the solid. Such a situation was realized by employing electrolytically sharpened tungsten needles. For the tungsten-InSb structure, for instance, a strong anomaly in the first derivative of the current-voltage characteristic was observed at 0.21 eV, which is in good agreement with the data on the fundamental absorption edge of this semiconductor.

EXPERIMENTAL RESULTS

At room temperature the electrical resistivity along the c axis, ρ_c , for different series of single crystals, varies between 100 and 180 $\Omega \cdot \text{cm}$. At 100 K the value of ρ_c becomes as high as 10^{10} – 10^{12} $\Omega \cdot \text{cm}$. A characteristic feature of the temperature dependence of the resistivity of CuO is the behavior of $\log \rho$ in the temperature range associated with magnetic phase transitions, 212 and 230 K (Fig. 1). Here, in contrast to the usual situation with semiconductors, the activation energy ε_a grows as the temperature drops below T_{N_1} and T_{N_2} . Near room temperature, ε_a ranges from 0.12 to 0.16 eV for different samples. Below 212 K the value of ε_a grows to 0.28–0.30 eV. Such a behavior of $\log \rho$ near T_{N_1} has also been observed in some transition-metal oxides, say, NiO (Ref. 9). A transitory region in which the $\log \rho$ vs T^{-1} plot is not a straight line is observed in the 212–230 K range.

The electrical resistivity of single-crystal CuO is anisotropic, the ratios of the values of ρ along the c , a , and b axes are 1:1.5:2.5. The $\log \rho$ vs T^{-1} curves for different axes are similar to each other (see Fig. 1), and the temperature dependence of the anisotropy of the resistivity of CuO is weak. According to the sign of the electromotive power, CuO possesses hole conductivity. Estimates place Hall's hole mobility μ in CuO below $0.05 \text{ cm}^2 \text{ V}^{-1} \text{ s}^{-1}$, which is lower than the carrier mobility of high- T_c superconductors and agrees with the values of μ in typical oxides of $3d$ -metals of the NiO type. Magnetoresistance in CuO is also low ($< 10^{-4}$ – 10^{-5}).

Measurements of the frequency dependence of σ in CuO show that in the 10^6 – 10^7 Hz range the conductivity rises somewhat as the frequency grows. At 300 K the ω -dependence of σ (the dispersion law) is insignificant, but as the temperature drops, σ increases with ω and can be ap-

proximately described by a $\sigma \propto \omega^n$ dependence with $n \leq 1$. Such a dependence, as is known, is associated with hopping calculation.¹¹ In the vicinity of T_{N_1} , the temperature dependence of $\sigma(\omega)$ undergoes the same drastic change as σ does in the dc mode. At such temperatures the values of $\sigma(0)$ and $\sigma(\omega)$ are close. As the temperature is lowered, $\sigma(\omega)$ becomes larger than $\sigma(0)$ and varies less rapidly. In the microwave range, $\sigma_{\text{mcw}} \approx \sigma(0)$ if $\sigma(0) \geq 5 \times 10^{-3} \Omega^{-1} \text{ cm}^{-1}$. At lower temperatures, when $\sigma(0) \leq 5 \times 10^{-3} \Omega^{-1} \text{ cm}^{-1}$, we found that $\sigma_{\text{mcw}} > \sigma(0)$ or even $\sigma_{\text{mcw}} \gg \sigma(0)$, and the conduction activation energy in the microwave mode was much lower than for $\sigma(0)$ (6 meV to 100 meV for different samples). At high temperatures $\Delta E_{\sigma_{\text{mcw}}} \approx \Delta E_{\sigma(0)} \approx 0.12$ – 0.16 eV. The change $\Delta E_{\sigma_{\text{mcw}}}$ occurs at a temperature close to T_{N_1} . On the whole, the above results concerning σ_{mcw} may also suggest that hopping conduction is present.¹¹

The sign of the thermopower $\alpha(T)$ corresponds (for all measured single-crystal and polycrystal samples) to p -type carriers, while its value is 100–200 $\mu\text{m K}^{-1}$ and is characterized by a slight temperature dependence. For CuO it has proved impossible to isolate a segment in the α vs T dependence with a specific activation energy, that is, a segment where the α vs T^{-1} dependence is linear. On the whole, however, this latter dependence is weaker than $\log \rho(T^{-1})$. This could point to the presence of a hopping-conduction activation energy in the temperature dependence of the electrical conductivity. Single crystals also exhibit a small peak in the α vs T dependence near T_{N_1} .

The dispersion law for light-induced conductivity, $\sigma(\omega)$, in the infrared range ($\omega = 0.08$ – 0.41 eV) for single-crystal CuO measured at 300 and 80 K, is depicted in Figs. 2 and 3, respectively. We see that at both temperatures the σ vs ω curve has the same shape: a broad Gaussian maximum at 0.22 eV and a narrower peak at 0.11 eV. At 300 K the intensity of the broad maximum is somewhat higher than at 80 K. The narrow peak at 300 K is more intense than that at 80 K by a factor of almost two, and their position on the energy scale is practically the same. The width of the broad maximum may be estimated at 0.20–0.25 eV, and the narrow peak is roughly 0.04 eV wide.

The measured dispersion of the reflection coefficient for single-crystal CuO, needed for calculations of the refractive

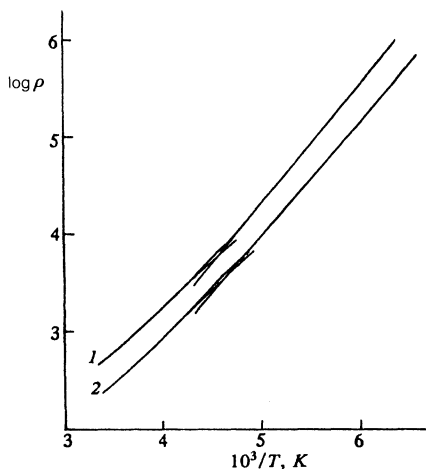


FIG. 1. The temperature dependence of electrical resistivity of a CuO single crystal: curve 1, along the b axis, ρ_b ; and curve 2, along the c axis, ρ_c .

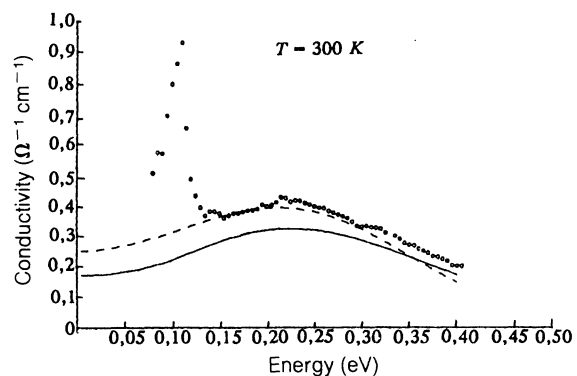


FIG. 2. Light-induced conductivity of single-crystal CuO in the infrared range at 300 K: the \circ represent the experimental data, the dashed curve corresponds to the calculation via (1), and the solid curve to the calculation via (2).

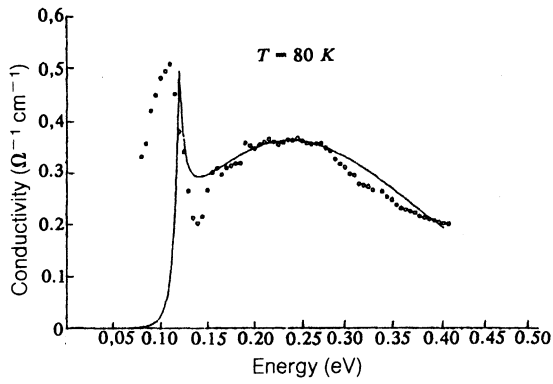


FIG. 3. Light-induced conductivity of single-crystal CuO in the infrared range at 80 K: the O represent the experimental data, and the solid curve corresponds to the calculation via (2).

index and, correspondingly, the light-induced conductivity in the 0.1–1.5 eV range, is listed in Ref. 4, where it is shown that R monotonically increases from 0.07 at 0.1 eV to 0.25 at 1.5 eV.

Figure 4 shows the resultant tungsten-needle-CuO-plane microjunction structure, the first derivative dU/dI of the current-voltage characteristic as a function of the applied electric field. Three anomalies can clearly be observed: a large one at 1.4 eV, which corresponds to the fundamental absorption edge of CuO (Ref. 12), and two others at 0.3 eV and at 0.9 eV. The peak at 0.3 eV with a width of 0.25–0.3 eV is comparable to the peak in the light-induced conductivity in the infrared, which has similar parameters.

4. DISCUSSION

The above results of optical and electrical measurements in CuO can be explained by the model of semiconductors with low charge-carrier mobility.^{9,13} The assumption that CuO is a semiconductor with low charge-carrier mobility is supported by the following facts: the low carrier mobil-

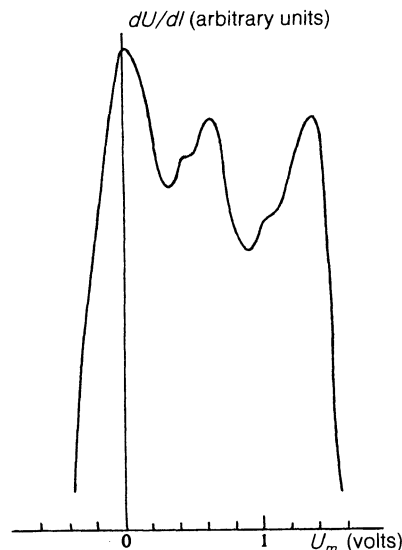


FIG. 4. The first derivative of the current-voltage characteristic of the microjunction tungsten-CuO structure as a function of the electric field at 300 K.

ity ($\ll 1 \text{ cm}^2 \text{ V}^{-1} \text{ s}^{-1}$), the absence of a measurable magnetoresistance, a dispersion law for the conductivity at moderate frequencies, $\sigma \propto \omega^n$ with $n \leq 1$, associated with hopping conduction, and, finally, the presence of a broad Gaussian peak in the light-induced conductivity in the infrared.

According to the theory,^{9,13} one of the most representative manifestations of low-mobility carriers (small polarons or of the small-polaron type) is the presence of a peak in the light-induced conductivity, due to a light-induced nonactivation transition of a polaron from one site to a neighboring site.

The theory of small-radius uncorrelated polarons yields the following expression for this peak in the light-induced conductivity:^{9,13}

$$\sigma(\omega, T) = \sigma(0, T) \frac{\sinh(2\Gamma\omega\tau_0)}{2\Gamma\omega\tau_0} \exp(-\omega^2\tau_0^2), \quad (1)$$

where ω is the light frequency, $\Gamma = \hbar\beta/4\tau_0$, $\beta = (kT)^{-1}$, $\tau_0 = t_0/4$ with $t_0 \approx \hbar(E_u/kT)^{0.5}$ the duration of a “jump,” and E_u the activation energy of small-polaron mobility.

According to this theory, the position of the absorption peak $\hbar\omega_{\text{max}}$ is related to the mobility activation energy E_u through the following formula: $\hbar\omega_{\text{max}} = 4E_u$. The width of the peak is $4\sqrt{E_u kT}$ in the high-temperature range $T > T_0 = \hbar\omega_{L0}/2kT \ln^4 \gamma$, where ω_{L0} is the frequency limit of longitudinal optical phonons, and $\gamma = 2E_u/\hbar\omega_{L0}$ the electron-phonon coupling parameter. At low temperatures ($T < T_0$) the width of the peak is $4\sqrt{E_u \hbar\omega_{L0}/2}$. The binding energy of a small-radius polaron, E_p , is approximately $2E_u$. From the position and width of the peak in the light-induced conductivity and the above formulas one can extract information about the carrier parameters of CuO. For instance, the small-polaron mobility activation energy $E_u \approx \hbar\omega_{\text{max}}/4 = 0.055 \text{ eV}$, the small-polaron binding energy $E_p \approx 2E_u = 0.11 \text{ eV}$, the electron-phonon coupling parameter $\gamma = E_p/\hbar\omega_{L0} \approx 1.6$ ($\hbar\omega_{L0} \approx 0.077 \text{ eV}$ for CuO; see Ref. 14), and the width of the light-induced conductivity peak is in the 0.20–0.25 eV range, which agrees fairly well with the values calculated by the above formulas at both high and low temperatures.

The small-polaron theory^{9,13} also implies that another manifestation of carriers of this type is the maximum in the dc conductivity as a function of the electric field at the same energy as does the peak in the light-induced conductivity. The respective expression closely resembles the formula for light-induced conductivity of small polarons, where $\hbar\omega$ is replaced by eEa , with e the electron charge, E the electric field strength, and a the length of the path of an accelerated electron.¹³

Further development of the small-electron theory and the effect of the theory on transport phenomena were first qualitatively discussed in Ref. 15. The theory of small polarons incorporating correlations was developed in Ref. 16. According to it, the hopping conductivity of small polarons is described by the

$$\sigma_h(\omega) = \sigma_h \frac{A(\omega)}{A(0)} \frac{\sinh(\beta\omega/2)}{(\beta\omega/2)} (1 + b_0)^{-0.25} \exp\{-\omega^2\tau_h^2 r_0(\omega)\}, \quad (2)$$

where

$$\sigma_h = (2\pi)^{0.5} R_1^{-1} e^2 t^2 \beta \tau_h A(0) \exp\{-2S_0 \text{th}(\beta\omega_0/4)\},$$

$$\tau_h = \sqrt{\sinh\left(\frac{\beta\omega_0}{2}\right) S_0^{-1} (2\omega_0)^{-1}},$$

$$A(\omega) = y^9 + y^4 + \frac{3}{2} (3 + 2y^2) [B_1(\omega) + B_{-1}(\omega)] \\ + 3y^2 [B_2(\omega) + B_{-2}(\omega)] \\ + \frac{1}{2} y^4 [B_1(\omega) + B_{-1}(\omega)] (2D^2)^{-1},$$

$$B_n(\omega) = (1 + b_n^2)^{0.25} (1 + b_n^2)^{-0.25} \\ \exp\{-\tau_h^2 [(\omega + nu_1)r_n(\omega) - \omega^2 r_0(\omega)]\},$$

$$b_n = 2\omega_0 \tau_h^2 (\omega + nu_1),$$

$$r_n(\omega) = 2\omega_0^{-1} \ln[b_n + (1 + b_n^2)^{0.5}] - 2b_n^{-2} [(1 + b_n^2)^{0.5} - 1],$$

with ω the photon energy (in electron volts), $\beta = (kT)^{-1}$, ω_0 the energy limit of longitudinal optical phonons (in electron volts), S_0 a parameter related to the energy u_1 of the interaction between neighboring small polarons with ϵ_∞ via the formula $S_0 = 10.3/\epsilon_\infty - 2.13u_1$ (Ref. 16), ϵ_∞ the high-frequency dielectric constant, R_1 the distances between the nearest neighbors (Cu^{2+} ions), and t the integral of transport between these ions.

The procedure for comparing the theoretical predictions [Eq. (2)] and the experimental data has been described in detail by Ihle and Lorenz¹⁶ as applied to Fe_3O_4 . In our case the best agreement between the theoretical and experimental curves representing the σ vs ω dependence was obtained for the following CuO parameters: $\omega_0 = 0.077$ eV (Ref. 14), $\epsilon_\infty = n^2 = 5.8$ (Refs. 4 and 12), $R_1 = 2.88$ Å (Ref. 4), and $t = 0.0018$ eV.

The first three parameters, ω_0 , ϵ_∞ , and R_1 , were taken from the cited experimental papers, and the transport inte-

gral t , which determines the width of the polaron conduction band in CuO, was varied to achieve agreement between the theoretical and experimental curves. When the magnitude of t was varied by $\mp 10\%$, the above agreement worsened considerably.

The results of comparison of the computer-calculated values of the light-induced conductivity in the infrared range by both theories [allowing for correlations, Eq. (2), and without correlations, Eq. (1)], at 300 K and 80 K are depicted in Figs. 2 and 3, respectively. The reader can see that both theories describe fairly accurately the broad maximum at 0.22 eV, while the narrow maximum at 0.11 eV, corresponding to E_p (the polaron binding energy), is described by the theory that allows for correlations.

Bearing in mind the values E_u and E_p for the charge carriers in CuO obtained from the frequency dependence of the light-induced conductivity, the reader can see that the sum $E_u + E_p = 0.055 + 0.11 \approx 0.165$ eV agrees fairly well with the dc-conduction activation energy, which varies between 0.12 and 0.16 eV depending on nonstoichiometry and the impurities in the sample.

Measurements of the first derivative of the current-voltage characteristic of the tungsten-CuO microjunction structure also support the assumption about the low-mobility carriers of the small-polaron type in CuO (Fig. 4). The diagram shows that at an energy of 0.3 eV the first derivative of the current-voltage characteristic possesses an anomaly corresponding to the maximum in the dc differential conductivity as a function of the electric field, similar to the maximum in the frequency dependence of the light-induced conductivity in the infrared range mentioned earlier. The width of this maximum is close to 0.2 eV. That the peak lies somewhat higher than 0.22 eV can be explained by the fact that the transitions caused by ballistic carriers are accompanied by momentum exchange and, hence, are indirect. As noted earlier, the presence of such a conductivity maximum

TABLE I. Semiconductor parameters of CuO.

1.	Electrical conductivity of undoped single crystals and polycrystals of CuO at 300 K at 100 K Electricity conductivity of $\text{Cu}_{0.99}\text{Li}_{0.01}\text{O}$ at 300 K at 100 K	$10^{-2} \Omega^{-1} \text{cm}^{-1}$ $10^{-12} \Omega^{-1} \text{cm}^{-1}$ $1 \Omega^{-1} \text{cm}^{-1}$ $10^{-7} \Omega^{-1} \text{cm}^{-1}$
2.	Conduction activation energy at 300 K at 100 K The ΔE_σ vs T^{-1} curve experiences a break at $T \approx T_N$	0.12–0.15 eV 0.25–0.30 eV
3.	Fundamental absorption edge	~ 1.4 eV (see Fig. 4 and Ref. 12)
4.	Thermopower A small temperature dependence is observed	$\sim 100 \mu\text{V K}^{-1}$
5.	For $T > T_N$, magnetoresistance is unmeasurable (less than 10^{-4})	
6.	dc dielectric constant	10.5
7.	High-frequency dielectric constant	5.8
8.	Limit energy of longitudinal optical phonons	~ 0.077 eV (Ref. 14)

TABLE II. The parameters of charge carriers in CuO.

1.	Concentration of charge carriers (holes) at 300 K	$\sim 10^{19} \text{ cm}^{-3}$
2.	Charge-carrier mobility at 300 K	$< 10^{-2} \text{ cm}^2 \text{ V}^{-1} \text{ s}^{-1}$
3.	Mobility activation energy of charge carriers in the hopping mode	0.055 eV
4.	Binding energy of charge carriers	0.11 eV
5.	Electron-phonon coupling parameter	1.6
6.	Characteristic times related to hopping and tunneling of charge carriers:	
	a) time between hoppings (lifetime in a localized state)	
	b) hopping time	$\Delta t = (\hbar^2/J^2 t_0)$
	c) tunneling percolation time	$\times \exp(E_u/kT)$ $t_0 \approx \hbar(E_u/kT)^{-0.5}$ $t_p = (\hbar/J) \exp \gamma$
At $T = 300 \text{ K}$, $E_u = 0.055 \text{ eV}$ and $J = 0.0018 \text{ eV}$ we have $\Delta t = 10^{-10} \text{ s}$, $t_0 \approx 10^{-14} \text{ s}$, and $t_p \approx 10^{-12} \text{ s}$.		

as a function of the electric field (and of the frequency) is, according to the theory, a characteristic manifestation of highly localized carriers. The strong anomaly in the first derivative of the current-voltage characteristic at 1.4 eV agrees well with the position of the fundamental semiconductor absorption edge in CuO (see, e.g., Ref. 12). Note that the nature of the anomaly at 0.9 eV is still unclear.

It may be added that the discovered frequency dependence of conductivity in the 10^6 – 10^7 Hz range of the $\sigma \sim \omega^n$ type with $n \leq 1$ for CuO samples with a conductivity $\sigma \leq 10^{-5} \Omega^{-1} \text{ cm}^{-1}$, the respective temperature dependence, and the results of studies of microwave conductivity, are associated with hopping conduction. This conclusion is also supported by the above-noted absence of a measurable magnetoresistance in CuO. The result corresponds to a low ($\ll 1 \text{ cm}^2 \text{ V}^{-1} \text{ s}^{-1}$) mobility of carriers in CuO.

Thus, the set of above experimental results on the optical and kinetic properties of CuO allows us to assume that CuO is a semiconductor with low-mobility carriers. The main semiconductor parameters of CuO and of small polarons in CuO are listed in Tables I and II.

When interpreting these results one must bear in mind that the general situation with the theory of magnetically ordered semiconductors with low-mobility carriers is complicated. It must be said that at present there is no meaningful theory that uses a unified model to consider the electrical and magnetic properties of magnetically ordered narrow-band semiconductor compounds of transition elements. The theory of small polarons (both correlated and uncorrelated) has been developed allowing for the possible effect of s - d exchange interaction. Nevertheless, as our results show, the theory of small polarons, which are formed only because of electron-phonon coupling, describes fairly well the maximum in the light-induced conductivity and other experimental results at reasonable values of all CuO parameters except one, the electron-phonon coupling parameter γ equal to 1.6. According to theoretical estimates, a typical small-radius polaron can be formed at $\gamma \sim 3$ – 4 . This estimate may be too high; a small polaron may be formed at lower values of γ . There is, however, another quite realistic possibility of formation of a small-radius polaron, namely, additional localization of an electron-phonon polaron due to electron-magnon coupling. It may be added that the shape of the peak

in the light-induced conductivity and the peak's parameters are practically independent of the nature of carrier localization, that is, as calculations show, they are practically the same for an electron-phonon polaron and an electron-magnon polaron. Hence, total electron-phonon-magnon interaction in CuO may form a highly localized low-mobility carrier of the small-polaron type.

Note that the sited parameters of carriers in CuO are very close to those in Fe_3O_4 (Ref. 16) and in ferrites,¹⁵ notwithstanding the marked difference in chemical composition and crystalline structures of these compounds. A sizable variation in the conduction activation energy at the Néel temperature in the antiferromagnet NiO (Ref. 9), proving that there is a strong link between conduction and magnetism, was observed not only in CuO. In a recent paper on the electrical properties of $\text{La}_2\text{CuO}_{4+y}$ (Ref. 17), a conclusion about the close relation between charge carriers and the magnetic state of this compound was drawn on the basis of the strong magnetoresistance effect measured in a magnetic field as high as 15 T.

Thus, the fairly narrow initial conduction bands for CuO and the sited $3d$ -oxides, antiferromagnetism, and the interaction of charge carriers with both phonons and magnons lead to localization and low mobility of the charge carriers.

In an earlier paper of ours³ dealing with the optical properties of $\text{YBa}_2\text{Cu}_3\text{O}_x$ with $6 \leq x \leq 7$ we observed, against the background of Drude absorption by free carriers, a similar broad maximum in the light-induced conductivity in the infrared. We concluded that there exists a combination of two types of carrier in this compound, band and hopping. In the case of CuO, apparently, there is only the conduction via low-mobility carriers of the small-polaron type. Carriers of this type may be assumed to play an important role in the formation of high- T_c superconductivity in the yttrium and lanthanum systems based on copper monoxide.

We are grateful to M. I. Klinger, É. L. Nagaev, and N. M. Plakida for useful discussions.

¹V. J. Emery, Phys. Rev. Lett. **58**, 2794 (1987).

²Yu. A. Izyumov, Usp. Fiz. Nauk **161**, No. 11, 1 (1991) [Sov. Phys. Usp. **34**, 935 (1991)].

³A. A. Samokhvalov, N. M. Chebotayev, N. N. Loshkareva, Yu. P. Suk-

- horukov *et al.*, Pis'ma Zh. Eksp. Teor. Fiz. **47**, 338 (1988) [JETP Lett. **47**, 404 (1988)].
- ⁴A. A. Samokhvalov, N. N. Loshkareva, Yu. P. Sukhorukov *et al.*, Pis'ma Zh. Eksp. Teor. Fiz. **49**, 456 (1989) [JETP Lett. **49**, 523 (1989)].
- ⁵Yu. A. Izyumov, I. M. Plakida, and Yu. I. Skryabin, Usp. Fiz. Nauk **159**, 621 (1989) [Sov. Phys. Usp. **32**, 1060 (1989)].
- ⁶T. I. Arbuzova, A. A. Samokhvalov, I. B. Smolyak, B. I. Karpenko *et al.*, J. Magn. Magn. Mater. **95**, 168 (1991).
- ⁷J. B. Forsyth, P. J. Brown, and B. M. Wähklun, J. Phys. C **21**, 2917 (1988).
- ⁸Yu. G. Naïdyuk and I. K. Yanson, *Microjunction Spectroscopy*, Znanie, Moscow (1989) [in Russian].
- ⁹*Polarons*, edited by Yu. A. Firsov, Nauka, Moscow (1975) [in Russian].
- ¹⁰B. A. Gizhevskii, A. A. Samokhvalov, N. M. Chebotaev *et al.*, Sverkhprovodimost' **4**, 827 (1991) [Superconductivity: Phys., Chem., Techn. **4**, 739 (1991)].
- ¹¹N. F. Mott and E. A. Davis, *Electronic Processes in Non-crystalline Materials*, Clarendon Press, Oxford (1979).
- ¹²L. V. Nomerovannaya, A. A. Makhnev, M. M. Kirillova *et al.*, Sverkhprovodimost' **3**, 169 (1990) [*sic*].
- ¹³M. I. Klinger, *Problems of Linear Electron (Polaron) Transport Theory in Semiconductors*, Pergamon Press, Oxford (1979).
- ¹⁴L. Degiorgi, E. Caldis, and P. Wachter, Physica C **153-155**, 657 (1988).
- ¹⁵M. I. Klinger and A. A. Samokhvalov, Phys. Status Solidi B **79**, 9 (1977).
- ¹⁶D. Ihle and B. Lorenz, J. Phys. C **19**, 5239 (1986).
- ¹⁷C. Y. Chen, R. J. Birgeneau, M. A. Kastner *et al.*, Phys. Rev. B **43**, 392 (1991).

Translated by Eugene Yankovsky